CHAPTER V

PARTIAL HYDROGENATION OF POLYUNSATURATED FATTY ACID METHYL ESTERS OVER Pd/ACTIVATED CARBON: EFFECT OF TYPE OF REACTOR

(Published in Chemical Engineering Journal, 210 (2012) 173–181)

5.1 Abstract

Partial hydrogenation of polyunsaturated FAMEs has been investigated on a Pd/C catalyst. The effect of type of reactor: batch and continuous flow reactors, on the FAME composition and properties of a biodiesel product were studied. In addition, many characterization techniques such as XRD, BET, FE-SEM, and CO-chemisorption were used to examine the prepared catalysts. The result showed that the partial hydrogenation of polyunsaturated FAMEs in a batch-type reactor provides higher selectivity towards C18:1 than that of a continuous-flow reactor. However, at the low conversion (78%); selectivity of C18:1 obtained from both types of reactors were almost the same.

Keywords: partial hydrogenation; Pd/activated carbon; biodiesel; oxidative stability; reactor.

5.2 Introduction

Biodiesel or fatty acid methyl ester (FAME) is known to be one of the most promising alternative fuels due to its biodegradability, lower emissions of SO_2, CO, un-burnt hydrocarbon and particulate matters, and higher cetane number as compared to petroleum-based diesel [1,2]. However, some biodiesel properties such as oxidative stability and cold flow properties depend on the natural characteristics of the starting oil [3]. Biodiesel produced from material that contains higher unsaturated fatty acid composition has a lower oxidative stability. In contrast, the higher the saturated fatty acid composition, the worse the cold flow property becomes. The oxidation of the unsaturated FAMEs produces peroxides, aldehydes, ketones, and acids that change biodiesel properties and affect the combustion process [4]. Therefore, the saturation of polyunsaturated FAMEs by partial hydrogenation is a promising way to improve its stability and enhance its utilization potential.

The catalysts used in commercial hydrogenation of triglycerides are usually Ni catalysts supported on silica or alumina, and mostly used in the slurry phases. These Ni catalysts are active in hydrogenation and cheaper than noble metal catalysts, but more severe hydrogenation pressure is required [5,6]. In this respect, noble metal catalysts such as Pd seem to be the most promising [7]. Pd supported on carbon materials has been extensively employed as a catalyst for hydrogenation reaction because of its advantages, e.g., high activity, mild process condition [8], availability of carbon support, and simplicity of recovery of Pd metal by just burning off the carbon component [9]. Several recent publications have addressed the activity of Pd supported on various types of carbon materials such as activated carbon [9–13], nanocomposite carbon [14], carbon nanofibers [15–17], and carbon nanotube [18]. Of the many types of carbon materials, activated carbon is still the most commonly used as a catalyst support, because of its large surface area (500–1,200 m^2/g) and low cost [19].

In addition, it is generally known that the type of reactor affects the conversion of the reactant and selectivity of the product after hydrogenation. Many researchers have investigated liquid-phase hydrogenation in a batch-type reactor [8,11,14,20,21] for the partial hydrogenation purpose, e.g., maximizing the

intermediate hydrogenated products and minimizing the deeply hydrogenated products. In a batch-type reactor where hydrogenation catalysts are used in the slurry phases, a stirrer could enhance the rate of reaction, but decrease the lifetime of the catalyst due to mechanical damages [22,23]. This attrition of catalysts will also cause some problems in the filterability of hydrogenated products. However, liquid-phase hydrogenation in a fixed-bed reactor has not been widely studied. The advantages of fixed-bed reactors are easy separation of the catalyst and products, and lowering mechanical damage of the catalyst particles.

On the basis of these facts, this study focused on the improvement of oxidative stability of biodiesel by partial hydrogenation of polyunsaturated FAMEs over Pd/activated carbon. In order to investigate the influence of the reactor type on the FAME composition and properties of the hydrogenated biodiesel product, two types of reactors, batch and continuous flow reactors, were studied. Moreover, details of the characterization of the Pd/C catalyst by XRD, BET, FE-SEM, and CO-chemisorption techniques were also reported.

5.3 Experimental

5.3.1 Materials

A commercial activated carbon purchased from Fluka Company with a BET surface area of 836.6 m^2/g and particle size $\leq$40 μm was used as a support. Palladium (II) nitrate dihydrate [$Pd(NO_3)_2.2H_2O$] 40% purum was purchased from Sigma Aldrich and used as a Pd precursor.

Gases used in the partial hydrogenation experiment were high purity (99.99%) hydrogen, and high purity (99.99%) nitrogen supplied from Thai Industrial Gases Public Co., Ltd. The biodiesel used in this work was obtained from Veerasuwan Co., Ltd., Thailand. In addition, tetrahydrofuran (stabilizer free, Wako) was used as a solvent for GC.

5.3.2 Catalyst Preparation

The 2 wt.% Pd on the activated carbon catalyst was prepared by incipient wetness impregnation (IWI) using a $Pd(NO_3)_2.2H_2O$ precursor. Firstly,

activated carbon was dried in an oven at 110°C for 24 h to remove the absorbed water. Secondly, the activated carbon was impregnated with a solution of Pd precursor for 24 h at room temperature to ensure that Pd diffused and dispersed thoroughly on the surface of the activated carbon. After that, it was dried in an oven at 110°C for 24 h. Finally, the dried catalyst was calcined at 500°C for 2 h under a nitrogen flow.

5.3.3 Catalyst Characterization

In order to identify the internal structure and crystallinity of the support and catalysts, a Rigaku DMAX2200 X-ray diffractometer was used. CuK_{α} radiation (1.5405 Å) was used as an X-ray source at running conditions, for the X-Ray tube, of 40 kV and 30 mA. The detector scanned the intensity of diffracted radiation from the sample as a function of 2-Theta in the range of 5° to 90° with a scan speed of 5°/sec.

The specific surface area, pore volume, and pore size distribution of the support and catalysts were determined by N_2 physisorption using a Quantachrome Autosorb-1 MP surface area analyzer. Before analyzing, the sample was heated in a vacuum atmosphere at 250°C overnight to eliminate volatile species that adsorbed on the surface.

Pd dispersion of the prepared catalysts was determined by pulse chemisorption of 10% CO/He at 50°C, using Temperature-Programmed Desorption/Oxidation/Reduction (TPD/R/O) Ohkura R6015. Prior to measurements, each sample was pretreated with hydrogen at 120°C for 1 h and followed by purging with helium at the same temperature for 10 min. The Pd dispersion was calculated by assuming a stoichiometry of CO:Pd = 1:1.

Furthermore, a Field Emission-Scanning Electron Microscope (FE-SEM), Hitachi Model S4800, was utilized to identify the microstructure and capture a micrograph of the catalyst morphology. The distribution of the Pd particle size was determined by using Semaphore®.

5.3.4 Partial Hydrogenation of Polyunsaturated FAMEs

5.3.4.1 *Batch-Type Reactor*

Partial hydrogenation of polyunsaturated FAMEs was carried out in a 300 ml stainless steel semi-batch reactor at a temperature and hydrogen partial pressure of 120°C and 0.4 MPa, respectively. Stirring rate was maintained at 500 rpm and the flow rate of hydrogen gas was 50 ml/min. Firstly, 1.5 g of Pd/C catalyst was placed into the reactor. Then, the system was purged with nitrogen to remove the remaining air. After that, 100 g of feed biodiesel was fed into the reactor by a peristaltic pump. The reaction was started by increasing the temperature and pressure to the desired point. Finally, the liquid products were collected every 30 minutes. The schematic of the partial hydrogenation experiment in batch-type reactor is shown in Figure 5.1(a).

5.3.4.2 *Continuous Flow-Type Reactor*

The experiments were performed using a stainless steel up-flow reactor (Figure 5.1(b)) at a temperature range of 80 to 120°C and hydrogen partial pressure of 0.1–0.4 MPa. The flow rate of hydrogen gas was fixed at 200 ml/min and was controlled by a mass flow controller. First, the Pd/C catalyst (0.2 g) was mixed with methyl cellulose and silica diluents. After that, the mixture was pressed and sieved to 600 μm–150 mm, and packed inside the reactor. Blank tests using methyl cellulose and silica diluents were run. It was confirmed that almost no hydrogenation reactions occurred within the experimental conditions. Second, the reactor was assembled to the system and pressurized to the desired pressure. After that, the temperature was increased to the desired point and was controlled by a temperature controller. Then, the feed biodiesel was passed through the catalyst bed by a high pressure pump with a flow rate in the range of 20–180 g/h. Finally, the liquid products were collected every hour for 5 h of reaction.

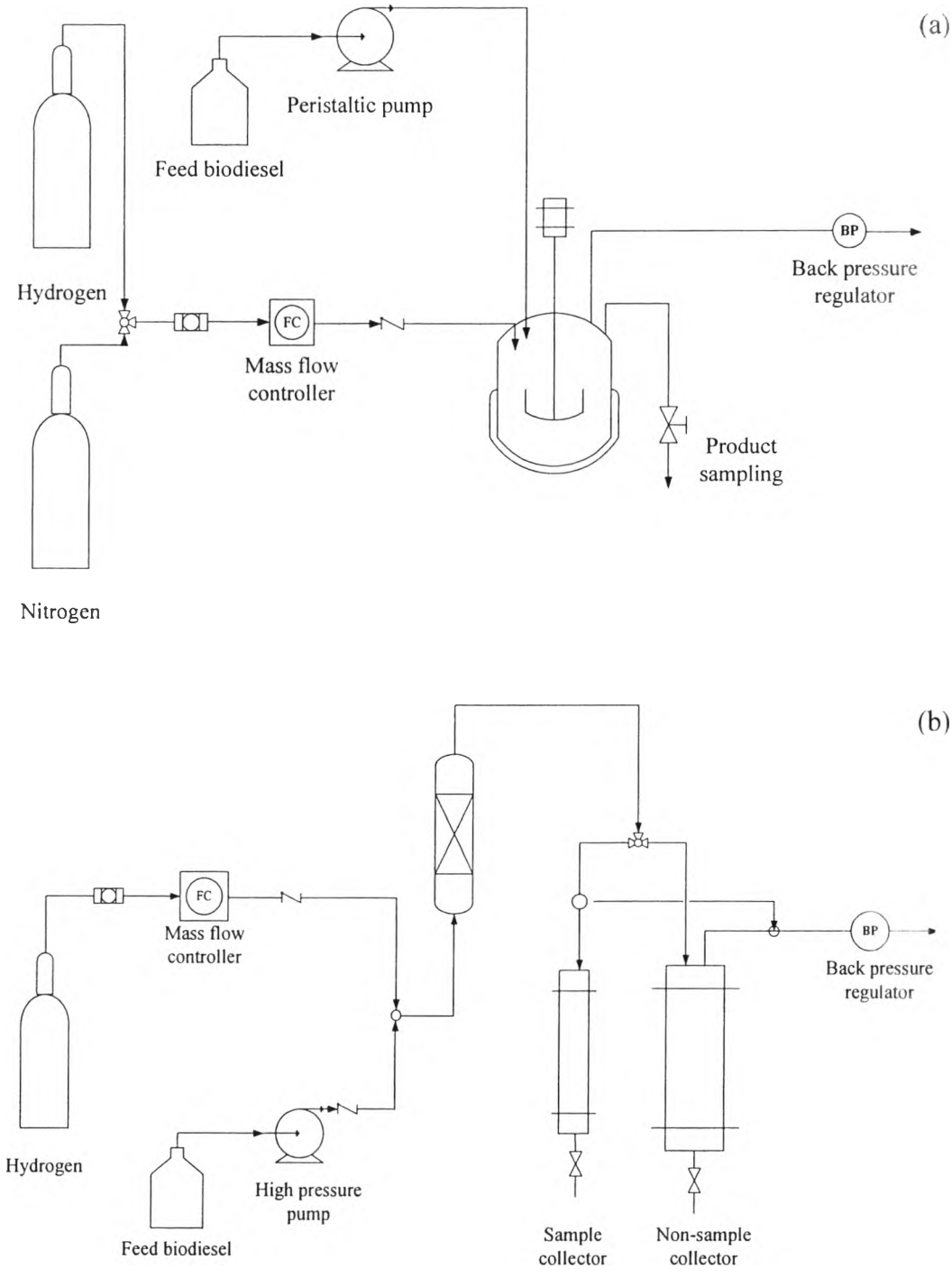

Figure 5.1 Schematic of partial hydrogenation in batch-type, (a) and continuous flow-type reactor, (b)

FAME composition in the biodiesel before and after the partial hydrogenation reaction was determined by using a Hewlett Packard gas chromatograph 6890N equipped with a flame ionization detector (GC-FID). A HP-88 (100 m x 250 μm x 0.2 μm) capillary column was used. Samples of 1 μl were injected under the following conditions: the carrier gas was helium with a flow rate of 2.4 ml/min, the injector temperature was 200°C with a split ratio of 75:1 and the detector temperature was 230°C. The sample was injected at an oven temperature of 155°C. After an isothermal period of 20 min, the GC oven was heated to 230°C at a rate of 2°C/min and held for 2.5 min with the total running time of 60 min. FAME composition was identified by reference to the retention time.

In addition, a Thermo Nicolet Fourier Transform-Infrared spectrometer (FT-IR) Nexus 670 was used to identify the chemical functional groups of biodiesel before and after partial hydrogenation, in order to confirm the results obtained from GC that the characteristic peak, which represents C=C disappeared after the biodiesel was partially hydrogenated. The liquid sample was placed on a Zn-Se sample holder. The IR spectra at 2 cm^{-1} resolution with 32 scans were collected in the range of 3,600 to 650 cm^{-1}.

Oxidative stability is one of the major issues indicating the content of polyunsaturated FAMEs. The oxidative stability of feed and hydrogenated biodiesel was tested by a Metrohm 743 Rancimat. Sample was aged at 110°C under a constant air stream. The oxidative stability corresponds to the period of time before FAMEs are degraded to such an extent that the formation of volatile acids can be recorded through an increase in conductivity. This procedure was developed according to EN 14112 [24].

Cold flow properties of biodiesel before and after partial hydrogenation including cloud point and pour point were investigated by using a Tanaka mini pour/cloud point tester Series MCP-102, which was developed according to ASTM D6749.

5.4 Results and Discussion

5.4.1 Catalyst Characterization

The characteristics of the prepared catalysts were obtained using various analytical techniques: XRD, BET, FE-SEM, and CO-chemisorption. A suitable calcination condition was already studied by our group [25]. The effect of catalyst calcination environment (air and N_2), calcination temperature (300°C and 500°C), and form of catalyst used in the reaction (as-received and reduced form) were investigated. It was found that different calcination conditions exhibit different Pd particle size, which plays an important role in the activity of the catalyst. The as-received form of catalyst calcined under N_2 at 500°C for 2 h with ~17 nm Pd particle size, provided a good catalytic activity for partial hydrogenation of polyunsaturated FAMEs. Therefore, the calcination procedure using N_2 at 500°C for 2 h was used. The presence of crystalline Pd after calcination of Pd/C catalyst was confirmed by XRD, as shown in Figure 5.2(b). The four main characteristic peaks of crystalline Pd including plane (111), (200), (220), and (311) at 2θ of 40.20, 46.80, 68.25, and 82.10, respectively, were observed. According to Wu *et al.* [26]; Pd (111), Pd (200), Pd (220), and Pd (311) were found after Pd/activated carbon fibers were calcined under N_2 atmosphere. In addition, the broad signal at about 25°, which is assigned to the amorphous carbon, was also observed in the activated carbon support (Figure 5.2(a)) and the Pd/C catalyst (Figure 5.2(b)) [27]. In order to evaluate hydrogenation activity of the prepared catalyst, the mean particle size of Pd was calculated from the peak width at half height of the Pd(111) diffraction peak by applying Scherrer's equation [9], the mean Pd particle size was 17.75 nm. After that, FE-SEM was subsequently employed in order to investigate the microstructure and morphology of the catalyst. FE-SEM micrograph of the Pd/C catalyst presented many small particles of Pd with a spherical shape; highly disperse on the surface of the activated carbon support (Figure 5.3). The average Pd particle size was 14.50 nm, which gave a result in agreement with the crystallite size calculated from XRD. Yeung *et al.* [28] also studied the crystallite size of Pt supported on highly oriented pyrolytic graphite by scanning tunneling microscope and found that the crystallite size of Pt is between 10–20 nm. In addition, Pd dispersion and Pd particle size were further identified by

the CO-chemisorption technique, which were 2.81% and 17.30 nm, respectively. It was shown that Pd particle sizes obtained from those three techniques were in agreement. These comparisons also indicated that there would be a small number of very small Pd particles over the Pd/C catalyst, which would be detected by CO-chemisorption but not detected by FE-SEM or XRD.

Surface area, total pore volume, and average pore diameter of the activated carbon support were analyzed by using an Autosorb-1 MP surface area analyzer. The surface area of activated C was 836.6 m^2/g, with the total pore volume of 0.5871 ml/g, and an average pore diameter of 2.307 nm. It could be suggested that almost all of the Pd particles could migrate from the inside pores of carbon to the outer surface of carbon during the calcination of Pd precursors.

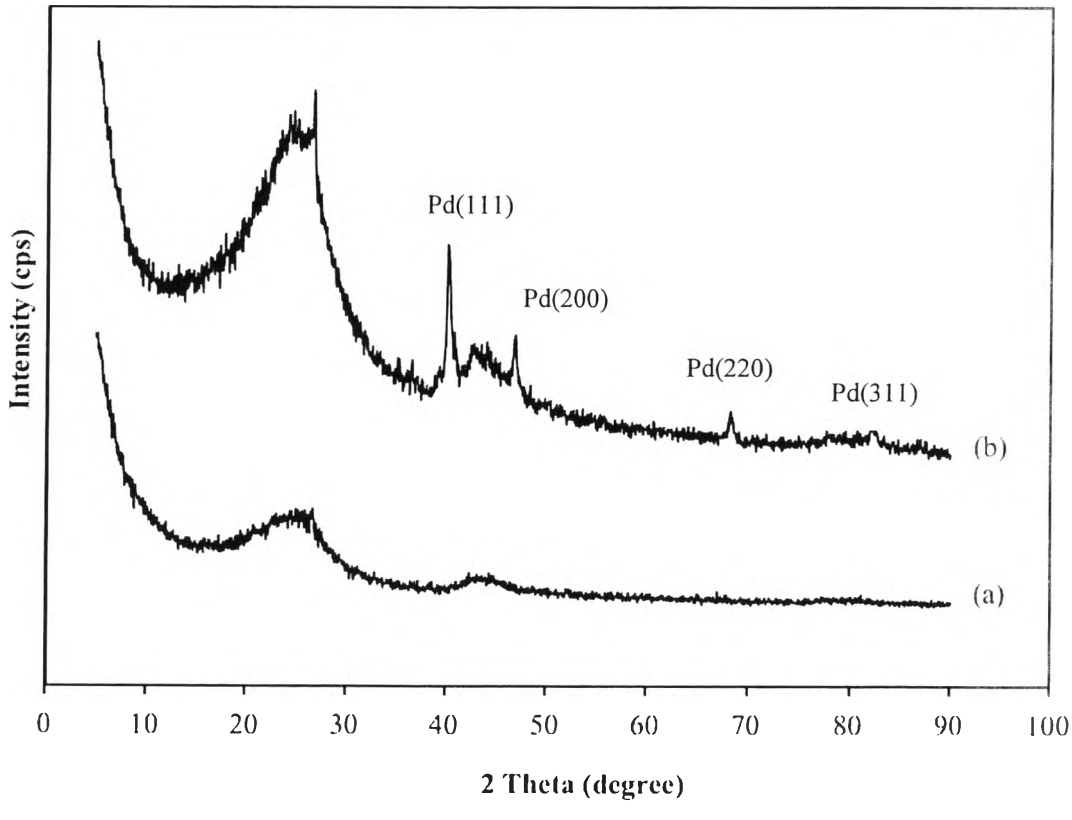

Figure 5.2 XRD patterns of activated carbon support, (a) and Pd/C catalyst calcined under N_2 at 500°C, (b).

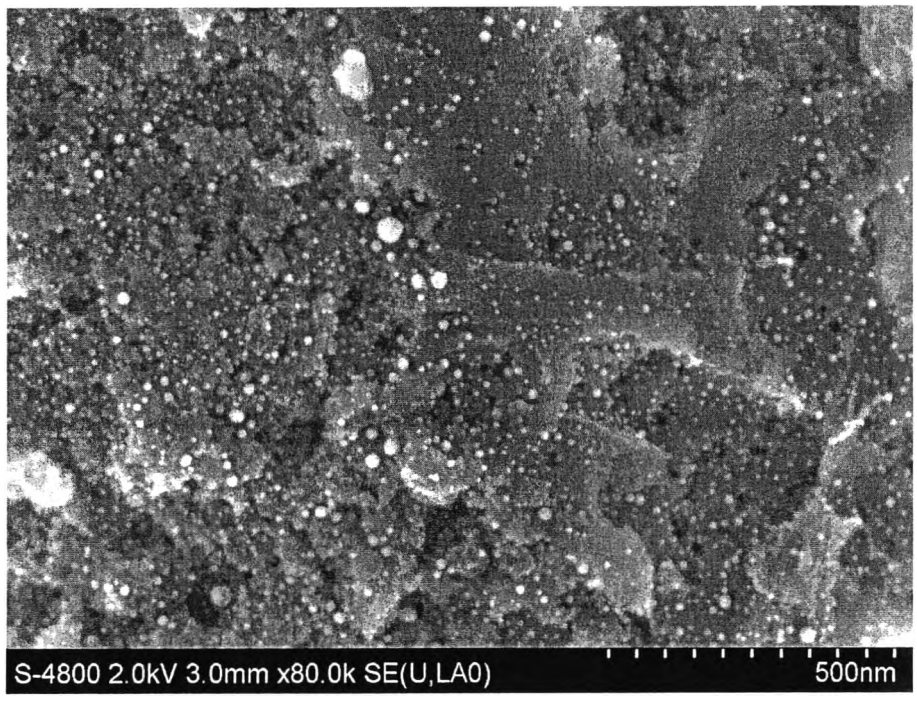

Figure 5.3 FE-SEM micrograph of Pd/C catalyst

5.4.2 Partial Hydrogenation of Polyunsaturated FAMEs in a Batch-Type Reactor

In order to evaluate the performance of the catalysts, the partial hydrogenation of biodiesel was operated and controlled at a condition of 120°C, 0.4 MPa, 50 ml/min hydrogen flow rate, 500 rpm stirring rate, and 1.5 wt.% of catalyst compared to the starting oil.

The percentages of C18:0, C18:1, C18:2, C18:3, and other FAMEs (C12:0, C14:0, C16:0, C16:1, C17:0, C20:0, C20:1, C22:0 and C24:0) before and after partial hydrogenation reaction are shown in Figure 5.4(a). It evidently showed that the higher the reaction time, the higher the conversion of unsaturated FAMEs (C18:3, C18:2, and C18:1) while the other FAMEs composition was quite stable. As shown in Figure 5.4(a), C18:3 and C18:2 were gradually hydrogenated as they decreased from 0.08% to 0.02% and 6.12% to 1.33%, respectively; whereas C18:1 and C18:0 increased from 29.93% to 32.44% and 4.90% to 7.01%, respectively, after 1 h of reaction. After that, at 1.5 h of reaction; C18:3 and C18:2 were completely hydrogenated as there were no significant compositions of them in the biodiesel

product; while a decreasing in composition of C18:1 due to its hydrogenation to C18:0 could be observed. This suggests that this Pd/C catalyst seems to meet the purpose in the partial hydrogenation point of view, which showed the behavior of consecutive reactions from C18:3 to C18:2, C18:2 to C18:1, and then C18:1 to C18:0, consequently. Many researchers [3,29,30] suggested that the higher the amount of saturated FAME, the higher oxidative stability was, and a worse cold flow property resulted. This suggests that the biodiesel product after 1.5 h of reaction would exhibit good fuel properties, especially oxidative stability and cold flow properties; where polyunsaturated FAMEs (C18:3 and C18:2) were fully converted to monounsaturated FAME (C18:1) with a minimal increase of saturated FAME (C18:0). The FAME composition and some fuel properties of biodiesel feed and biodiesel product after 1.5 h of batch reaction are reported in Table 5.1. It demonstrates that partial hydrogenation can improve the oxidative stability of biodiesel from 1.49 h to 32.50 h, which meets the Thai Standard, which requires ≥10 h of oxidative stability even without addition of any antioxidants. However, the hydrogenated biodiesel exhibited an unfavorable pour point and cloud point, which shows a limitation in cold flow properties of hydrogenated biodiesel. However, this problem can be minimized by blending with petroleum diesel in a proper composition [31].

Another interesting observation is an increase of *trans*-C18:1 composition with the reaction time as presented in Figure 5.4(b). This indicates that some of the unreacted *cis*-C18:1 are transformed into *trans*-C18:1 under this pressure and temperature [11]. This result is consistent with the work done by Agustin and co-workers [32]. They found that hydrogenation and *cis-trans* isomerization of the C=C bonds simultaneously take place during the hydrogenation of vegetable oil or FAMEs.

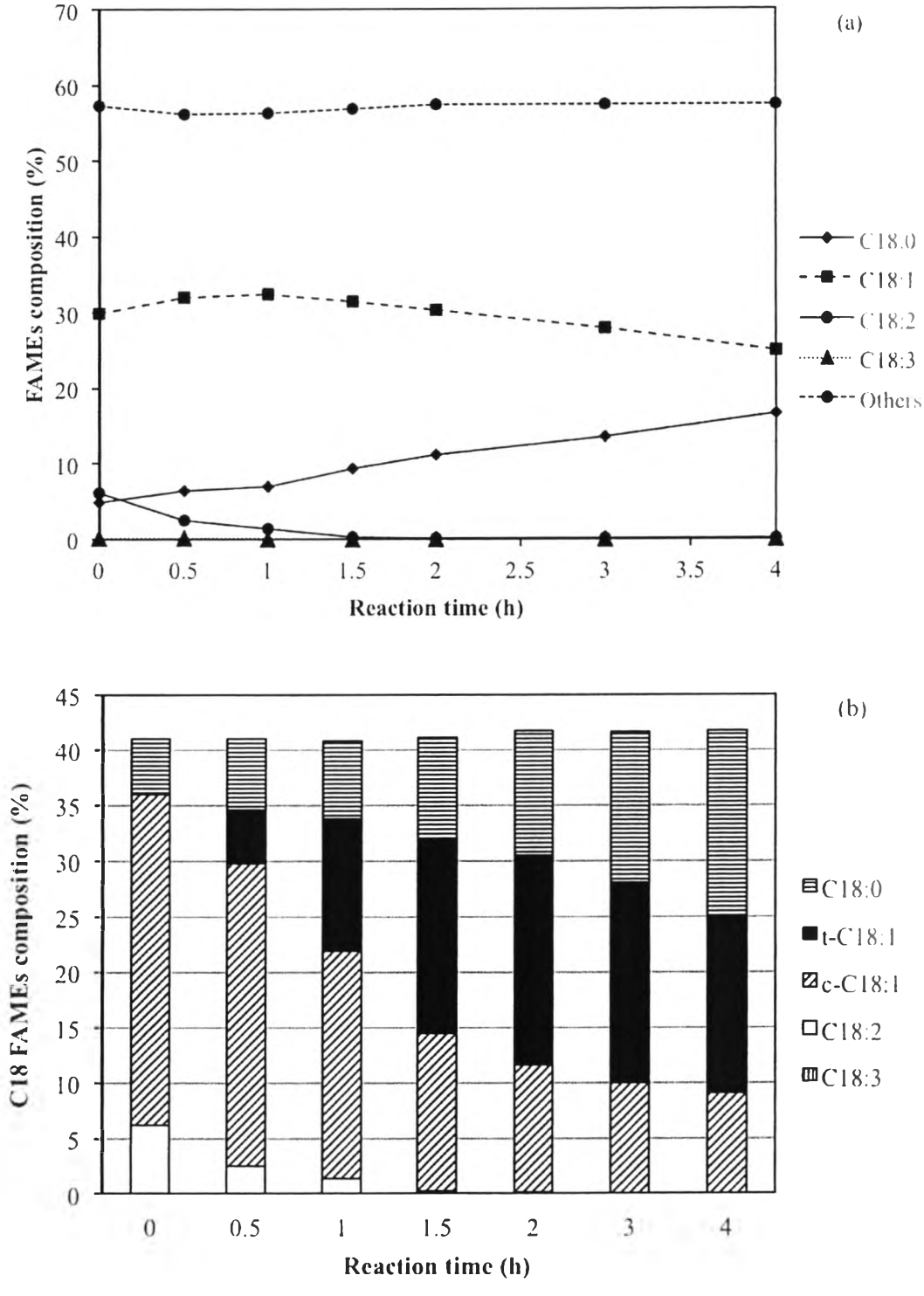

Figure 5.4 Total FAMEs, (a) and C18 FAMEs composition, (b) of biodiesel after partial hydrogenation in a batch-type reactor as a function of reaction time (Reaction conditions: 120°C, 0.4 MPa, 50 ml/min H_2 flow rate, 500 rpm stirring rate, and 1.5 wt.% catalyst compared with starting oil)

Table 5.1 FAMEs composition and some fuel properties of biodiesel feed and biodiesel product after 1.5 h of hydrogenation in a batch-type reactor.

	Biodiesel feed	**Biodiesel product after 1.5 h**
FAMEs Composition (%)		
Saturated FAMEs	61.92	66.01
Monounsaturated FAMEs	30.12	31.63
trans-Monounsaturated FAMEs	0.11	17.36
cis-Monounsaturated FAMEs	30.01	14.27
Diunsaturated FAMEs	6.12	0.31
Triunsaturated FAMEs	0.08	0.00
Fuel Properties		
Oxidative stability (h)	1.49	32.50
Pour point (°C)	16.0	22.0
Cloud point (°C)	16.0	23.0

Figure 5.5(a) shows an FT-IR spectrum of biodiesel feed. The peak at 3006 cm^{-1} corresponding to =C–H stretching in *cis*-configuration indicates the presence of unsaturated FAMEs, where nearly all of the double bonds in the biodiesel feed are in the *cis*-form [33]. The peaks at 1742 and 1169 cm^{-1}, which corresponds to C=O stretching and (C=O)–O stretching of FAME were also detected, respectively [34]. Figure 5.5(b) shows the disappearance of a peak of =C–H stretching at 3006 cm^{-1} in the biodiesel product with an increase in hydrogenation time: 0, 0.5 1.5, and 3 h in a batch reactor. The disappearance of this peak monitors the saturation of double bond during hydrogenation reaction and the isomerization of remaining double bonds in the original *cis*-form. This explanation can be confirmed by the appearance of the peak at 966 cm^{-1} after partial hydrogenation, as shown in Figure 5.5(c), which can be attributed to C–H out of plane in *trans*-configuration [35]. It is clearly seen that the peak intensity of *trans*-configuration at 966 cm^{-1}

increased with hydrogenation time; that is consistent with the results obtained from GC.

Moreover, it was found that the correlation between the logarithm of the ratio of *cis/trans* C18:1 with the ratio of C18:2 & C18:3/C18:1 is linear (not shown here). This suggests that as C18:3 and C18:2 were hydrogenated to C18:1, a higher isomerization of *cis*-C18:1 to *trans*-C18:1 took place. This result is in accordance with the work done by Nikolaou and co-workers [4]; they found that C18:1 *cis/trans* ratio presented a high exponential correlation with the conversion during hydrogenation of sunflower oil using Rh sulfonated triphenylphosphite complexes. The trend of activity, selectivity, and *cis-trans* isomerization of precious metal catalysts has been reported by Dijkstra [36]. Pd, which is the most active metal, also causes the most *cis-trans* isomerization and migration of double bonds. The presence of *trans*-isomers leads to a much higher melting point than those of the corresponding *cis*-isomers [37]. The melting point of *trans*-C18:1 is 9°C, whereas it is only -20°C for *cis*-C18:1 [38]. Therefore, for our future work, we will modify the catalysts to minimize the *trans*-isomers formation for improving the cold flow properties of the partially hydrogenated products.

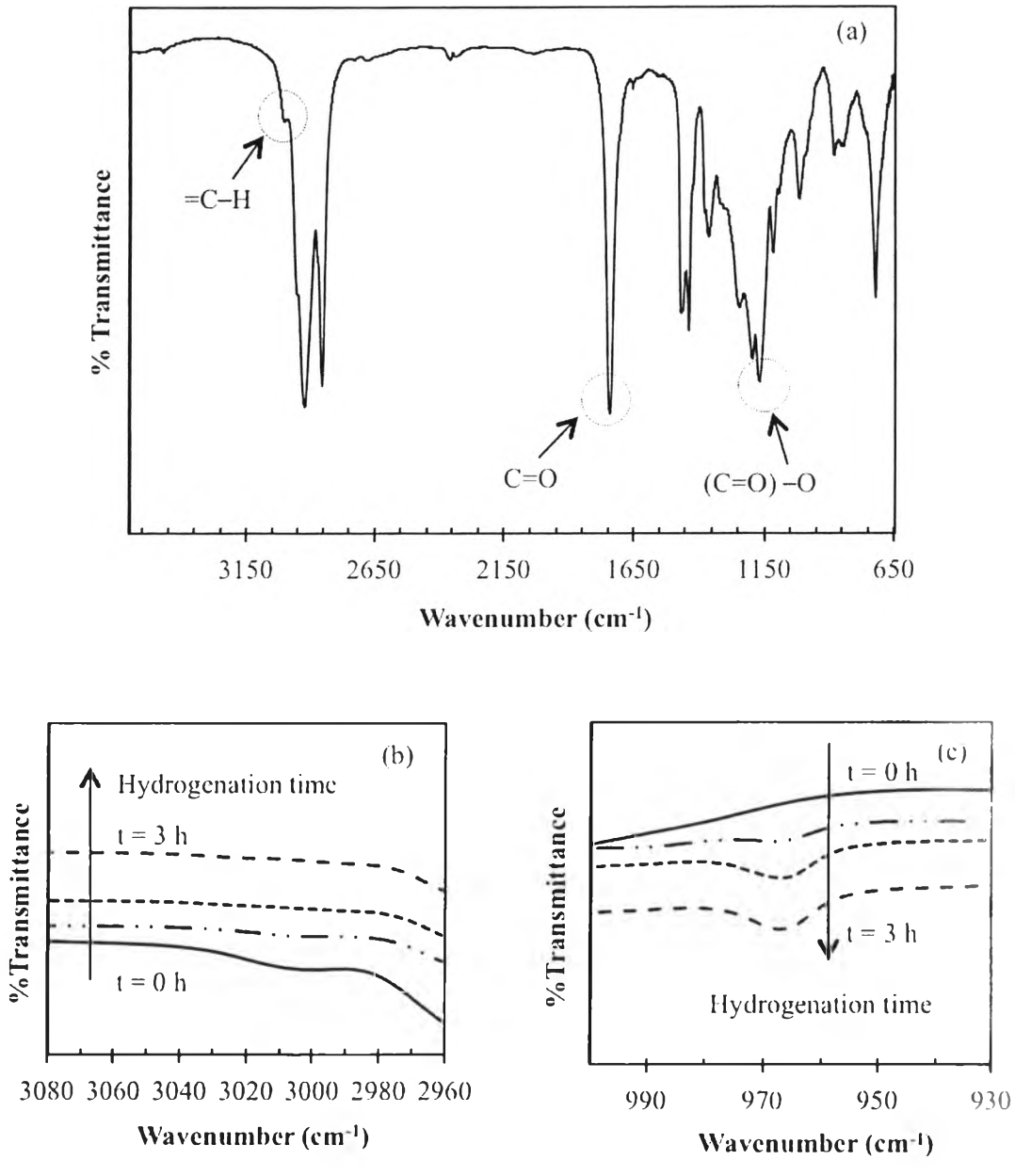

Figure 5.5 FT-IR spectra of (a) biodiesel feed, (b) =C–H stretching, and (c) C–H out of plane in *trans*-configuration in biodiesel product after partial hydrogenation in a batch reactor at 0, 0.5, 1.5, and 3 h.

5.4.3 Partial Hydrogenation of Polyunsaturated FAMEs in a Continuous Flow Reactor

The partial hydrogenation of polyunsaturated FAMEs in a continuous flow reactor was conducted at various parameters: reaction temperature, hydrogen partial pressure, and biodiesel feed flow rate.

5.4.3.1 Effect of Reaction Temperature

To study the effect of temperature; hydrogen partial pressure, hydrogen flow rate, and biodiesel feed flow rate, respectively, were fixed at 0.4 MPa, 200 ml/min, and 90 g/h, while the reaction temperature was varied from 80 to 120°C. It was found that the conversion of C18:2 and C18:3 increased with the higher reaction temperature. The conversions of C18:2 and C18:3 at 80°C, 100°C, and 120°C were 53%, 66%, and 73%, respectively. Figure 5.6 shows that the increase in temperature caused an increase of *trans*-C18:1 and C18:0. This was due to the transformation of *cis*-C18:1 to *trans*-C18:1 as the result of the higher temperature and higher reaction rate at the higher temperature according to kinetics principle.

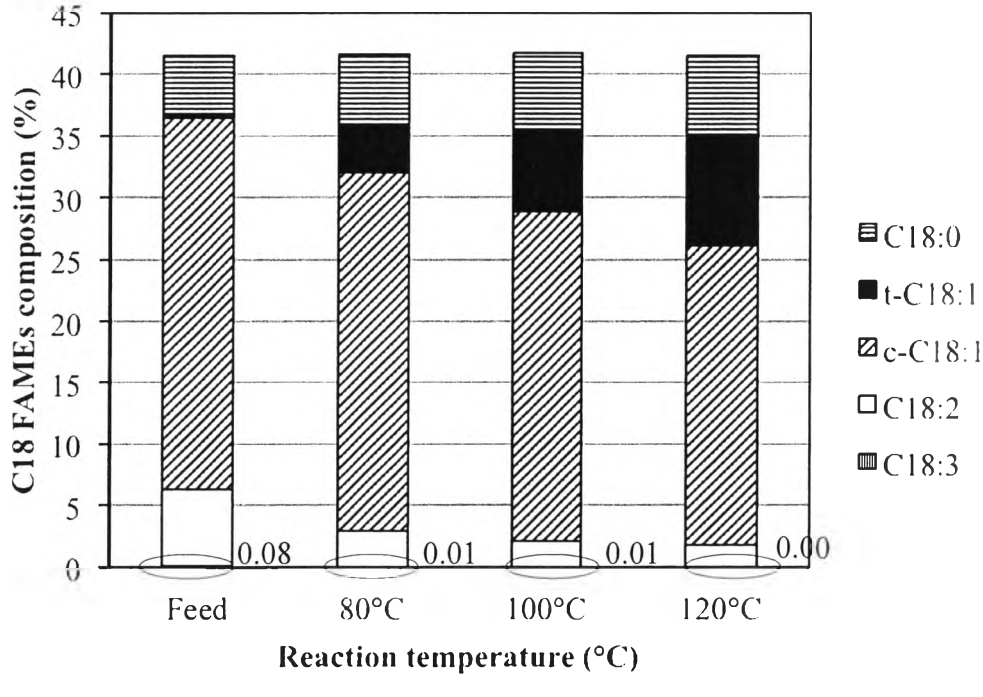

Figure 5.6 Effect of reaction temperature on composition of C18 FAMEs (Reaction conditions: 0.4 MPa, 200 ml/min H_2 flow rate, and 90 g/h biodiesel feed flow rate)

5.4.3.2. Effect of Hydrogen Partial Pressure

The effect of hydrogen partial pressure was investigated by varying hydrogen partial pressure from 0.1 to 0.4 MPa; whereas temperature, hydrogen flow rate, and biodiesel feed flow rate were fixed at 120°C, 200 ml/min, and 90 g/h, sequentially. Hydrogen partial pressure also had a significant effect on the conversion of polyunsaturated FAMEs. With the hydrogen partial pressure being increased from 0.1 to 0.4 MPa, the conversion of C18:2 and C18:3 increased. It was 55%, 60%, and 71% C18:2 and C18:3 conversion for 0.1 MPa, 0.2 MPa, and 0.4 MPa, respectively. This can be explained by the increase of hydrogen partial pressure that resulted in more presence of hydrogen, which caused the hydrogenation reaction to accelerate faster. Moreover, it showed that at a higher hydrogen partial pressure, the higher amount of *trans*-C18:1 and C18:0 was produced, as shown in Figure 5.7. This is due to the transformation of *cis*-C18:1 to *trans*-C18:1 under the higher pressure, which was in accordance with the result obtained at the higher reaction temperature.

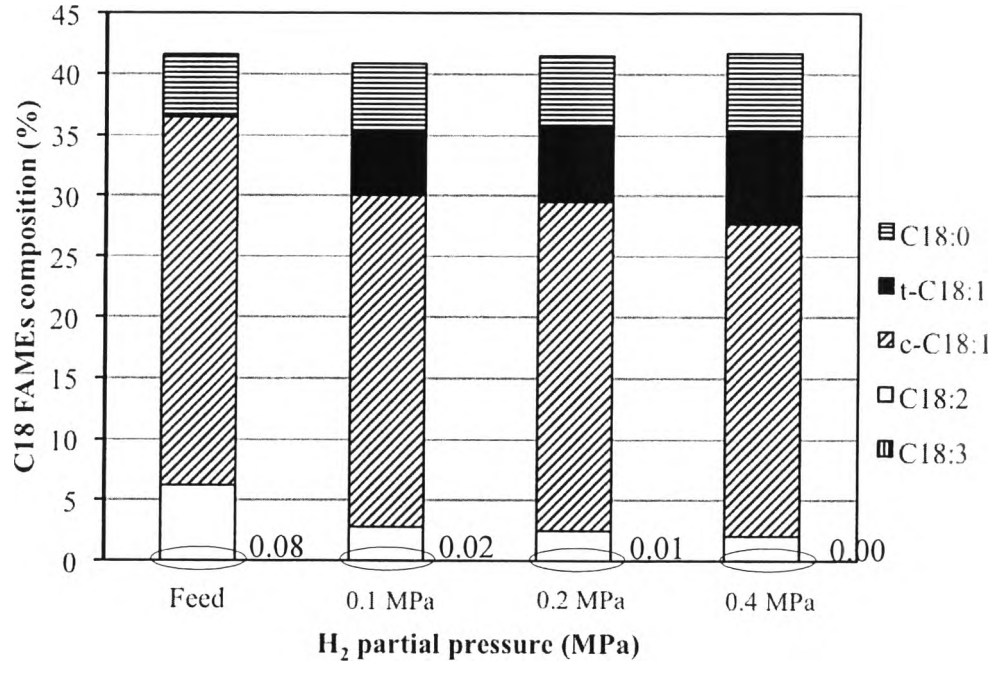

Figure 5.7 Effect of hydrogen partial pressure on composition of C18 FAMEs (Reaction conditions: 120°C, 200 ml/min H_2 flow rate, and 90 g/h biodiesel feed flow rate)

5.4.3.3 Effect of Biodiesel Feed Flow Rate

The biodiesel feed flow rate was varied from 20 to 180 g/h; where the other parameters were fixed at 120°C, 0.4 MPa of hydrogen partial pressure, and a 200 ml/min hydrogen flow rate. As shown in Table 5.2, the conversions in a continuous flow reactor were equivalent to that in the batch reactor, even at the short contact time, i.e., average contact time of 0.01 h for the biodiesel flow rate of 20 g/h, using 0.2 g of Pd/C catalyst. On the contrary, 100 g of biodiesel was hydrogenated over 1.5 g of Pd/C catalyst within the reaction time of 2 h in a batch reactor. These data suggest that continuous flow reactor was more preferable than the batch-type reactor in terms of the hydrogenation-processing rate per unit amount of Pd/C catalyst. Figure 5.8 shows a comparison of C18 FAMEs as a function of contact time. With an increase in contact time, the amount of C18:3 and C18:2 gradually decreased, whereas the amount of *trans*-C18:1 and C18:0 increased. Deeper hydrogenation of *trans*-C18:1 into C18:0 was significant under the longer contact time between the biodiesel and catalysts.

Table 5.2 C18:2 and C18:3 conversions of batch and continuous-flow reactor at different reaction and contact times.

Batch		**Continuous-flow**		
Reaction time (h)	Conversion (%)	Biodiesel feed flow rate (g/h)	Contact time (h)	Conversion (%)
0.5	58.6	180	0.0011	44.2
1	78.3	120	0.0017	57.2
1.5	94.5	90	0.0022	69.7
2	97.1	60	0.0033	77.5
3	97.9	50	0.0040	88.5
4	98.3	40	0.0050	90.9
		20	0.0100	96.2

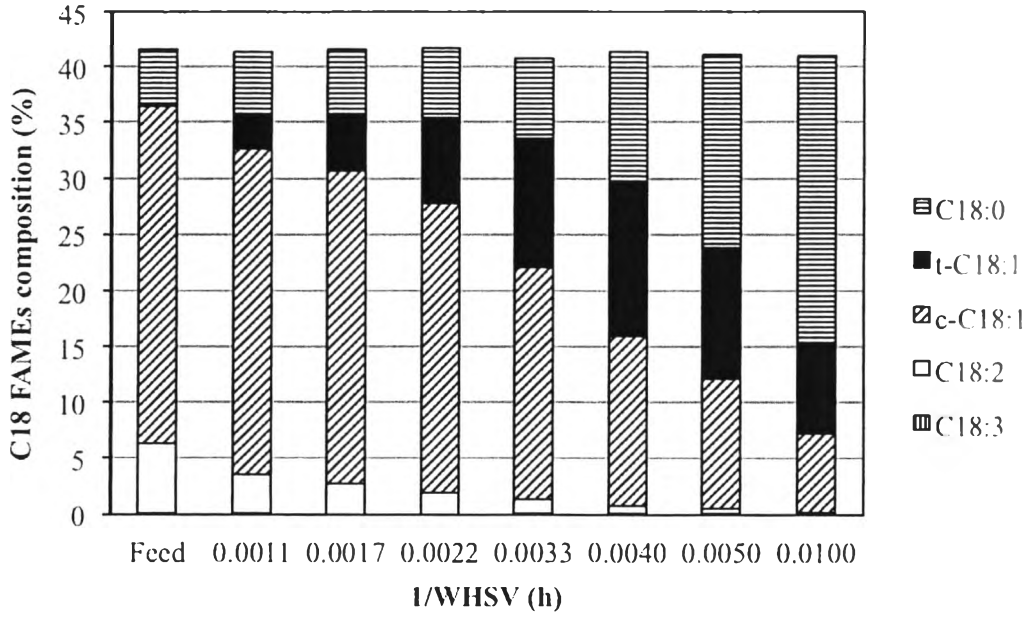

Figure 5.8 Effect of contact time (1/WHSV) on composition of C18 FAMEs (Reaction conditions: 120°C, 0.4 MPa, 200 ml/min H_2 flow rate)

The oxidative stability of biodiesel products obtained from different biodiesel feed flow rates were investigated. Figure 5.9(a) shows the oxidative stability as a function of composition of polyunsaturated FAMEs (C18:2 and C18:3). After hydrogenation; the composition of C18:2 and C18:3 decreased with an increase of oxidative stability. At the higher degree of hydrogenation (the lower biodiesel feed flow rate), the lower composition of C18:2 and C18:3 and resulted in higher oxidative stability. It could be suggested that to meet the Thai standard, which requires 10 h of oxidative stability; the composition of C18:2 and C18:3 should be less than 0.65%.

Moreover, cold flow properties of biodiesel as a function of saturated FAMEs (C18:0) composition in the biodiesel product, operated at different biodiesel feed flow rates, were also investigated as presented in Figure 5.9(b). With a higher degree of hydrogenation (utilizing a lower biodiesel feed flow rate), the higher composition of C18:0 and resulted in an increasing of cloud point and pour point.

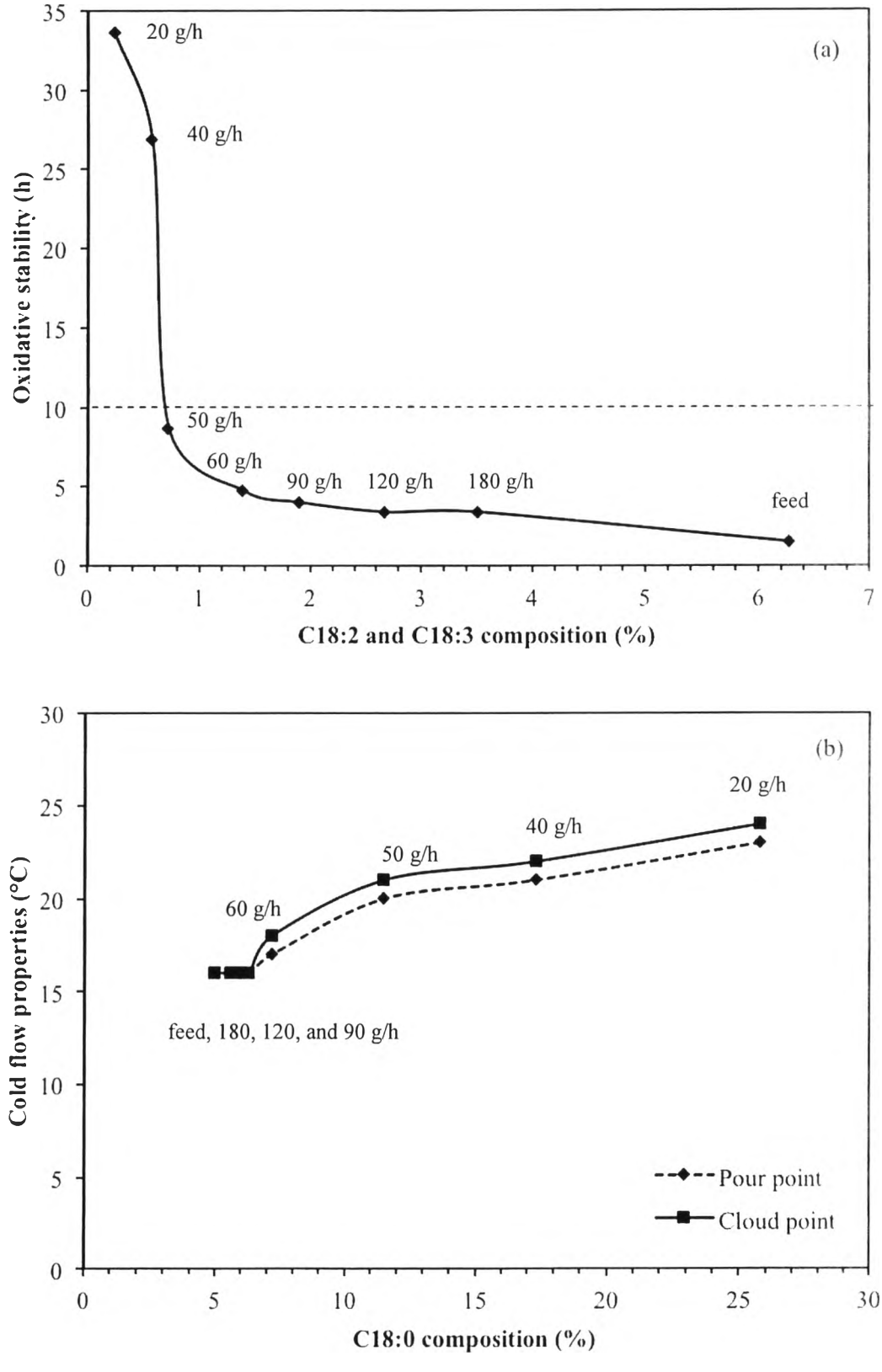

Figure 5.9 Oxidative stability (a) and cold flow properties (b) of biodiesel feed and biodiesel product operated at different biodiesel feed flow rates.

According to the above results, it could be concluded that reaction conditions of contact time of 0.004 h where biodiesel feed flow rate was 50 g/h and the amount of Pd/C catalyst was 0.2 g, would be optimal for partial hydrogenation in a continuous flow reactor, where we could obtain biodiesel products with oxidative stability that meet the Thai standard without the addition of any antioxidants. At this contact time, the biodiesel product composed of 11.5% of C18:0 with 20°C and 21°C pour point and cloud point, respectively. Therefore, the critical composition of C18 FAMEs to get biodiesel products that pass the Standard are as follows: C18:2 and C18:3 $\leq$ 0.65%, C18:1 $\geq$ 25%, and C18:0 $\leq$ 12%.

5.4.4 Difference in Catalytic Performances between a Batch-Type Reactor and Continuous-Flow Reactor

The catalytic performances of 2 wt.% Pd/C catalyst in a batch-type reactor and continuous-flow reactor were compared by fixing the reaction temperature and hydrogen partial pressure at 120°C and 0.4 MPa, respectively.

In order to compare the partial hydrogenation of polyunsaturated FAMEs in batch and continuous flow reactors, the FAME composition of biodiesel product at the same conversion were compared. Figure 5.10 displays the comparison of C18 FAMEs composition in the biodiesel feed and a biodiesel product obtained from batch and continuous-flow reactors at different conversions. At the lowest conversion of C18:2 and C18:3 (58%), selectivity of C18:1 obtained from the batch-type reactor and continuous flow reactor was almost the same, although the hydrogenation processing rate was $W_{BDF}/W_{cat}/\Delta t$ = 100g/1.5g/0.5h = 133 h^{-1} and WHSV = 120g/0.2g/1h = 600 h^{-1}, respectively. At the conversion of 78%, selectivity of C18:1 obtained from both types of reactor was still the same, even though the hydrogenation processing rate of the batch reactor ($W_{BDF}/W_{cat}/\Delta t$ = 100g/1.5g/1h = 67 h^{-1}) was lower than that of the continuous flow reactor (WHSV = 60g/0.2g/1h = 300 h^{-1}). On the other hand, at the conversion of 94%, a biodiesel product obtained from a batch-type reactor provided higher selectivity towards C18:1, whereas the hydrogenation processing rate of the batch and continuous flow reactors was $W_{BDF}/W_{cat}/\Delta t$ = 100g/1.5g/1.5h = 44 h^{-1} and WHSV = 40g/0.2g/1h = 200 h^{-1}, respectively.

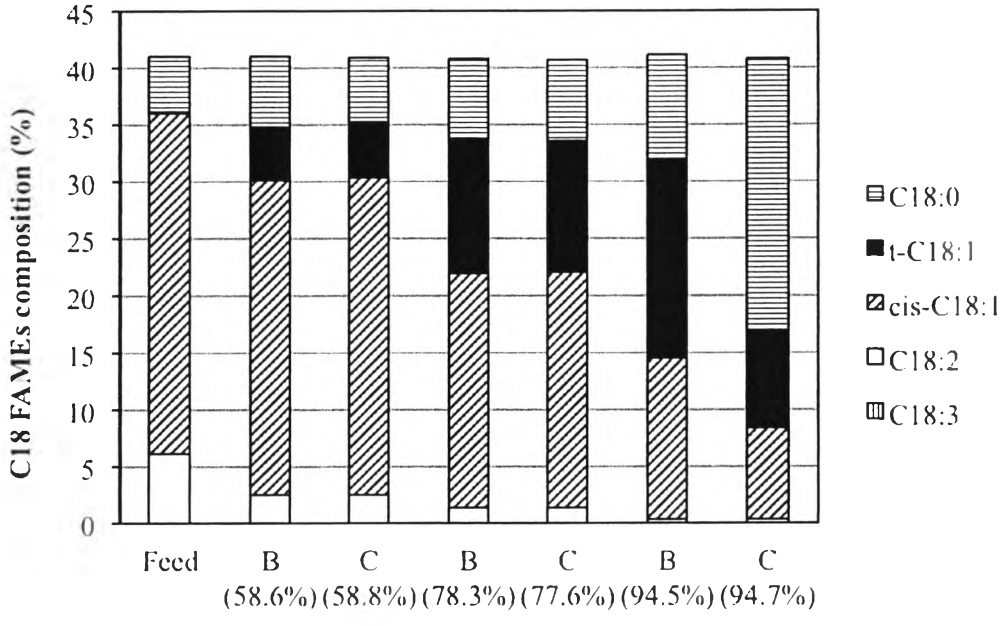

Figure 5.10 Comparison of C18 FAMEs composition of biodiesel feed and product obtained from batch (B) and continuous-flow (C) reactors at different conversions of C18:2 and C18:3.

This suggests that a continuous flow reactor could hydrogenate biodiesel about 4–5 times faster than a batch-type reactor. These differences in reactivity between a batch-type reactor and continuous flow reactor could be explained by the possibility of oil contact with the catalyst surface where molecular hydrogen is activated, i.e., more frequent contact in a continuous flow reactor and less contact in a batch reactor. This lesser contact could suppress the deeper hydrogenation of the hydrogenated intermediate products (C18:1) into saturated products (C18:0). This explanation can be confirmed from the higher selectivity towards C18:1 of the batch-type reactor at the conversion of 94%. Gómez-Quero *et al.* [39] also found that switching from a batch to continuous reactor resulted in an increase in hydrodechlorination rate of 2,4-dichlorophenol over Pd/Al_2O_3.

In addition, the selectivity of *cis*-C18:1 in biodiesel products obtained from batch and continuous flow reactors as a function of conversion of C18:2 and C18:3 was also considered (not shown here). It obviously presented that at higher C18:2 and C18:3 conversion, the lower cis-C18:1 selectivity was obtained. This was

due to the further hydrogenation of *cis*- and *trans*-C18:1 to C18:0 at higher C18:2 and C18:3 conversion. Furthermore, the results also showed that at the high conversion (>80%); the batch reactor provides higher selectivity towards *cis*-C18:1. Nevertheless, at the lower conversion; both types of reactor provide product with almost the same *cis*-C18:1 selectivity. This was consistent with the result of selectivity towards C18:1 obtained from both types of reactor, which could be explained by the different in contact probability between catalyst and oil in both types of reactor.

Thus, it can be suggested that, to obtain the high conversion and high selectivity towards C18:1 and *cis*-C18:1, the partial hydrogenation of polyunsaturated FAMEs in a batch-type reactor is better. However, to obtain the same selectivity at a lower conversion, operating in a continuous flow reactor is better because it requires much lower residence time when compared to a batch-type reactor.

5.5 Conclusions

Partial hydrogenation of polyunsaturated FAMEs has been investigated on a Pd/C catalyst. It was found that this catalyst provides good partial hydrogenation activity, which showed the behavior of consecutive reactions from C18:3 to C18:2, C18:1, and C18:0, resulting in an improvement of the oxidative stability. Moreover, the results showed that the type of reactor used had an important effect on the conversion and selectivity of C18:1. It was found that the partial hydrogenation in a continuous flow reactor provided hydrogenation rates 4–5 times higher than in a batch type reactor. However, the partial hydrogenation in a batch-type reactor provided higher selectivity towards C18:1 at a high conversion. This can be explained by the possibility of oil contact with the catalyst surface in a batch reactor being lower than that of a continuous flow reactor. This lesser contact between oil and catalyst in a batch type reactor would suppress the deeper hydrogenation of intermediate products (C18:1) into saturated products (C18:0). In contrast, at the lower conversion; selectivity of C18:1 obtained from both types of reactors were almost the same. In conclusion, it could be suggested that to obtain the high

conversion and high selectivity towards C18:1, partial hydrogenation of polyunsaturated FAMEs in a batch type reactor is better. However, to obtain the same selectivity at a lower conversion; operating in continuous flow reactor is better because it requires much lower residence time when compared to the batch-type reactor.

5.6 Acknowledgements

The authors gratefully acknowledge the financial support from the Chulalongkorn University Dutsadi Phipat Endowment Fund, Chulalongkorn University, Thailand, and Center of Excellence on Petrochemical and Materials Technology, Thailand.

5.7 References

[1] N. Ellis, F. Guan, T. Chen, C. Poon, Monitoring biodiesel production (transesterification) using in situ viscometer, Chem. Eng. J. 138 (2008) 200–206.

[2] Y.H. Taufiq-Yap, H.V. Lee, R. Yunus, J.C. Juan, Transesterification of non-edible Jatropha curcas oil to biodiesel using binary Ca–Mg mixed oxide catalyst: Effect of stoichiometric composition, Chem. Eng. J. 178 (2011) 342–347.

[3] T. Sonthisawate, A. Suemanotham, Y. Yoshimura, T. Makoto, Y. Abe, Upgrading of biodiesel fuel quality by partial hydrogenation Process, Global Warming Conference: Biodiversity and their Sustainable Use. (2009) 90–97.

[4] N. Nikolaou, C.E. Papadopoulos, A. Lazaridou, A. Koutsoumba, A. Bouriazos, G. Papadogianakis, Partial hydrogenation of methyl esters of sunflower oil catalyzed by highly active rhodium sulfonated triphenylphosphite complexes, Catal. Commun. 10 (2009) 451–455.

[5] H.W.B. Patterson, Hydrogenation of Fats and Oils: Theory and Practice, in: G.R. List, J.W. King (Eds.), 2nd ed., American Oil Chemist's Society Press, 2011, pp. 169–187.

[6] R.R. Allen, M.W. Formo, R.G. Krishnamurthy, G.N. McDermott, F.A. Norris. N.O.V. Sonntag, Bailey's Industrial Oil and Fat Products, in: D. Swern (Ed.), fourth ed., A Wiley-Interscience Publication, John Wiley & Sons, 1982, pp. 1–95.

[7] M. Zajcew, The hydrogenation of fatty oils with palladium catalyst IV. Pilot-plant preparation of shortening stocks, J. Am. Oil Chem. Soc. 37 (1960) 130–132.

[8] J. Panpranot, O. Tangjitwattakorn, P. Praserthdam, J.G. Goodwin Jr, Effects of Pd precursors on the catalytic activity and deactivation of silica-supported Pd catalysts in liquid phase hydrogenation, Appl. Catal. A. 292 (2005) 322–327.

[9] T. Harada, S. Ikeda, M. Miyazaki, T. Sakata, H. Mori, M. Matsumura, A simple method for preparing highly active palladium catalysts loaded on various carbon supports for liquid-phase oxidation and hydrogenation reactions, J. Mol. Catal. A: Chem. 268 (2007) 59–64.

[10] H. Tamai, U. Nobuaki, H. Yasuda, Preparation of Pd supported mesoporous activated carbons and their catalytic activity, Mater. Chem. Phys. 114 (2009) 10–13.

[11] K. Wadumesthrig, S.O. Salley, K.Y.S. Ng, Effects of partial hydrogenation, epoxidation, and hydroxylation on the fuel properties of fatty acid methyl esters, Fuel Process. Technol. 90 (2009) 1292–1299.

[12] L. Wang, X. Chen, J. Liang, Y. Chen, X. Pu, Z. Tong, Kinetics of the catalytic isomerization and disproportionation of rosin over carbon-supported palladium, Chem. Eng. J. 152 (2009) 242–250.

[13] P. Mäki-Arvela, G. Martin, I. Simakova, A. Tokarev, J. Wärnå, J. Hemming, B. Holmbom, T. Salmi, D.Yu. Murzin, Kinetics, catalyst deactivation and modeling in the hydrogenation of ß-sitosterol to ß-sitostanol over microporous and mesoporous carbon supported Pd catalysts, Chem. Eng. J. 154 (2009) 45–51.

[14] I.L. Simakova, O.A. Simakova, A.V. Romaneko, D.Y. Murzin, Hydrogenation of vegetable oils over Pd on nanocomposite carbon catalysts, Ind. Eng. Chem. Res. 47 (2008) 7219–7225.

[15] R.F. Bueres, E. Asedegbega-Nieto, E. Diaz, S. Ordonez, F.V. Diez, Preparation of carbon nanofibres supported palladium catalysts for hydrodechlorination reactions, Catal. Commun. 9 (2008) 2080–2084.

[16] J. Zhu, J. Zhou, T. Zhao, X. Zhou, D. Chen, W. Yuan, Carbon nanofiber-supported palladium nanoparticles as potential recyclable catalyst for the Heck reaction, Appl. Catal. A. 352 (2009) 243–250.

[17] D.B. Thakur, R.M. Tiggelaar, J.G.E. Gardeniers, L. Lefferts, K. Seshan. Carbon nanofiber based catalyst supports to be used in microreactors: Synthesis and characterization, Chem. Eng. J. 160 (2010) 899–908.

[18] C. Ge, Y. Li, J. Zhao, R. Zhou, Carbon nanotubes supported palladium catalysts for selective hydrogenation of cinnamaldehyde under atmospheric pressure, Indian J. Chem. 49A (2010) 281–287.

[19] M.L. Toebes, J.A.V. Dillen, K.P. de Jong, Synthesis of supported palladium catalysts, J. Mol. Catal. A: Chem. 173 (2001) 75–98.

[20] I.V. Deliy, N.V. Maksimchuk, R. Psaro, N. Ravasio, V.D. Santo, S. Recchia, E.A. Paukshtis, A.V. Golovin, V.A. Semikolenov, Kinetic peculiarities of *cis/trans* methyl oleate formation during hydrogenation of methyl linoleate over Pd/MgO, Appl. Catal. A. 279 (2005) 99–107.

[21] A.F. Perez-Cadenas, F. Kapteijn, M.P. Zieverink M, J.A. Moulijn, Selective hydrogenation of fatty acid methyl esters over palladium on carbon-based monoliths structural control of activity and selectivity, Catal. Today. 128 (2007) 13–17.

[22] J. Ni, F.C. Meunier, Esterification of free fatty acids in sunflower oil over solid acid catalysts using batch and fixed bed-reactors, Appl. Catal. A. 333 (2007) 122–130.

[23] N. Shibasaki-Kitakawa, H. Honda, H. Kuribayashi, T. Toda, T. Fukumura, T. Yonemoto, Biodiesel production using anionic ion-exchange resin as heterogeneous catalyst, Bioresour. Technol. 98 (2007) 416–421.

[24] M.J. Ramos, C.M. Fernandez, A. Casas, L. Rodriguez, A. Perez, Influence of fatty acid composition of raw materials on biodiesel properties, Bioresour. Technol. 100 (2009) 261–268.

[25] N. Numwong, A. Luengnaruemitchai, Y. Yoshimura, Effects of palladium precursor and catalyst calcination condition on the catalytic activity of activated

carbon-supported palladium in partial hydrogenation of polyunsaturated fatty acid methyl esters, Renewable Energy Conference (2010).

[26] X. Wu, N.C. Gallego, C.I. Contescu, H. Tekinalp, V.V. Bhat, F.S. Baker, M C. Thies, The effect of processing conditions on microstructure of Pd-containing activated carbon fibers, Carbon. 46 (2008) 54–61.

[27] H. Wu, L. Zhuo, Q. He, X. Liao, B. Shi, Heterogeneous hydrogenation of nitrobenzenes over recyclable Pd(0) nanoparticles catalysts stabilized by polyphenol-grafted collagen fibers, Appl. Catal. A. 366 (2009) 44–56.

[28] K.L. Yeung, E.E. Wolf, Scanning tunneling microscopy studies of size and morphology of Pt graphite catalysts, J. Catal. 135 (1992) 13–26.

[29] G. Knothe, Dependence of biodiesel fuel properties on the structure of fatty acid alkyl esters, Fuel Process. Technol. 86 (2005) 1059–1070.

[30] M.J. Ramos MJ, C.M. Fernández, A. Casas, L. Rodríguez, A. Pérez, Influence of fatty acid composition of raw materials on biodiesel properties. Bioresour. Technol. 100 (2009) 261–268.

[31] S. Goto, M. Oguma, N. Chollacoop, L. Dowling, D. Sheedy, W. Zhang *et al.*, EAS-ERIA biodiesel fuel trade handbook: 2010, 1st printed, Economic Research Institute for Asian and East Asia (ERIA), 2008.

[32] F. Agustin, C. Perez, M.P.Z. Martijn, K. Freek, A.M. Jacob, High performance monolithic catalysts for hydrogenation reactions, Catal. Today. 105 (2005) 623–628.

[33] S. GuO, K.Y. Liew, J. Li, Catalytic activity of ruthenium nanoparticles supported on carbon nanotubes for hydrogenation of soybean oil, J. Am. Oil Chem. Soc. 86 (2009) 1141–1147.

[34] N.P.G. Roeges, A guide to complete interpretation of infrared spectra of organic structures, John Wiley & Sons, Chichester, 1994.

[35] J. Fritsche, H. Steinhart, New techniques and applications in lipid analysis, in: R.E. McDonald, M.M. Mossoba (Eds.), American Oil Chemist's Society Press, Champaingn IL, 1997, pp. 234–255.

[36] A.J. Dijkstra, Revisiting the formation of *trans* isomers during partial hydrogenation of triacylglycerol oils, Eur. J. Lipid Sci. Tech. 108 (2006) 249–264.

[37] G. Knothe, "Designer" biodiesel: optimizing fatty ester composition to improve fuel properties, Energy Fuels. 22 (2008) 1358–1364.

[38] G. Knothe, R.O. Dunn, A comprehensive evaluation of the melting points of fatty acids and esters determined by differential scanning calorimetry, J. Am. Oil Chem. Soc. 86 (2009) 843–856.

[39] S. Gómez-Quero, F. Cárdenas-Lizana, M.A. Keane, Liquid phase catalytic hydrodechlorination of 2,4-dichlorophenol over Pd/Al_2O_3: Batch vs. continuous operation, Chem. Eng. J. 166 (2011) 1044–1051.